Optical Realization of Coherent Vibrational Dynamics in Molecules

Stefano Longhi

Dipartimento di Fisica and Istituto di Fotonica e Nanotecnologie del CNR, Politecnico di Milano, Piazza L. da Vinci 32, I-20133 Milano, Italy

Optical analogues of coherent vibrational phenomena in molecules, such as light-induced molecular stabilization and wave packet dynamics at a potential crossing, are proposed for light beams in coupled slab waveguides.

OCIS codes: 130.2790, 230.3120, 230.7370, 000.1600

Light propagation in coupled optical waveguides provides an excellent laboratory tool to visualize with classical waves the dynamical aspects embodied in a wide variety of coherent phenomena encountered in atomic, molecular or condensed-matter physics [1]. Among others, we mention adiabatic stabilization of atoms in ultrastrong laser fields [2], Bloch oscillations, Zener tunneling and dynamic localization in crystalline potentials [3–5], coherent population transfer in laser-driven atoms [6, 7], and quantum Zeno dynamics [8]. As compared to quantum systems, optics offers unique possibilities such as a direct visualization in space of typical ultrafast phenomena in

time and the ability to explore coherent dynamical regimes of difficult access in quantum systems or obscured by detrimental effects such as dephasing and particle-particle interaction. Previous optical analogies [1] deal with coupled channel waveguides in an assigned geometry, in which spatial light transport turns out to be analogous to the coherent evolution of a single-particle electronic wave function. Unfortunately, these photonic structures could not account for vibrational effects typical of e.g. molecules or crystals. Nuclear degrees of freedom in molecules are known to yield a wealth of interesting phenomena, especially when driven by ultrastrong laser fields. Coherent effects in molecules, like laser-assisted preparation and control of vibrational wavepackets and molecular bond engineering, provide theoreticians and experimentalists with examples of time-dependent quantum mechanics at work, with important applications to femtochemistry [9–11]. Though current pump-probe techniques enable the observation of time-resolved wave packet dynamics of nuclear motion, optical analogues of coherent vibrational phenomena may offer the possibility to assess wave packet dynamical phenomena of difficult access in the quantum realm, such as wave packet dynamics and momentum filtering at surface potential crossings [12].

In this Letter optical analogues of laser-assisted coherent vibrational phenomena in molecules, such as light-induced molecular stabilization and wave packet dynamics at surface potential crossings, are theoretically proposed for light beams propagating in coupled slab waveguides. The photonic structure, schematically shown in Fig.1(a), consists of two slab waveguides S_1 and S_2, placed at a distance d, which confine the

field in the transverse y direction. In the weak guidance approximation, light propagation at wavelength λ is described by the Schrödinger-like wave equation for the electric field envelope $\psi(x, y, z)$ [1, 13]

$$i\hbar\partial_z\psi = -[\hbar^2/(2n_s)]\nabla_t^2\psi + [n_s - n(x, y)]\psi \tag{1}$$

where $\nabla_t^2 = \partial_x^2 + \partial_y^2$ is the transverse Laplacian, $\hbar = \lambda/(2\pi) = 1/k$ is the reduced wavelength, n_s is the bulk refractive index, $n = n_s + \Delta n_1(x, y - d/2) + \Delta n_2(x, y + d/2)$ is the refractive index profile of the structure, and $\Delta n_{1,2}(x, y)$ are the refractive index increase in the two slab guiding regions. The index profiles $\Delta n_{1,2}$ are generally allowed to slowly vary along the horizontal x direction, such as in case of graded-index slabs or slabs with slowly-varying thickness [13]. We indicate by $q_1(y; x)$ and $q_2(y; x)$ the fundamental mode profiles of the two slabs at a given transverse coordinate x and by $W_{1,2}(x)$ the respective effective indices, i.e. $-(\hbar^2/2n_s)\partial_y^2 q_{1,2} + \Delta n_{1,2}(x, y)q_{1,2} = W_{1,2}q_{1,2}$. Assuming that $W_{1,2}(x)$ differ from a reference value W_0 by a small quantity (of order $\sim \epsilon^2$) and that the field ψ and the effective indices $W_{1,2}$ vary slowly with respect to x, a multiple-scale asymptotic analysis shows that the solution to Eq.(1) can be written as $\psi(x, y, z) = [\psi_1(x, z)q_1(y - d/2; x) + \psi_2(x, z)q_2(y + d/2; x)] \exp(-iW_0 z/\hbar) + O(\epsilon^2)$, where the slowly-varying amplitudes $\psi_{1,2}$ satisfy the coupled Schrödinger-like equations

$$i\hbar\partial_z\psi_{1,2} = -[\hbar^2/(2n_s)]\partial_x^2\psi_{1,2} + \mathcal{U}_{1,2}(x)\psi_{1,2} + \kappa(x)\psi_{2,1}. \tag{2}$$

In Eqs.(2), we have set $\mathcal{U}_{1,2} = W_{1,2}(x) - W_0 + \int dy \Delta n_{2,1} q_{1,2}^2 + (\hbar^2/2n_s) \int dy (\partial_x q_{1,2})^2 \simeq$

$W_{1,2}(x) - W_0$, $\kappa = \int dy \Delta n_1 q_1 q_2 = \int dy \Delta n_2 q_1 q_2$ and the normalization conditions $\int dy q_{1,2}^2 = 1$ have been assumed. In their present form, Eqs.(2) are analogous to the quantum mechanical equations describing the vibrational dynamics of a molecule onto two energy surfaces $\mathcal{U}_{1,2}$ coupled by an external laser field (interaction strength κ) in the Born-Oppenheimer and rotating-wave approximations (see, for instance, [9, 12]). Note that the temporal variable in the quantum problem is replaced here by the spatial propagation distance z, the reduced nuclear mass by n_s, the Planck constant by the wavelength λ, and the inter-nuclear distance by the coordinate x. This analogy enables to investigate in optics the classical analogues of a wide variety of wave packet phenomena encountered in molecular systems. We will limit here to discuss two of such analogies. The first one, shown in Fig.1(b), is the phenomenon of laser-induced stabilization of a dissociating molecule, which is usually explained by the formation of light-induced adiabatic surface potentials $\mathcal{U}_{\pm}(x)$, defined by the equation $\mathcal{U}_{\pm}^2 - (\mathcal{U}_1 + \mathcal{U}_2)\mathcal{U}_{\pm} - \kappa^2 + \mathcal{U}_1\mathcal{U}_2 = 0$ (see, for instance, [9, 14, 15]). Let us consider a diatomic molecule (like H_2^+) characterized by a bonding ($\mathcal{U}_1$) and an antibonding ($\mathcal{U}_2$) potential curve. A dissociating vibrational wave packet is initially created from the ground vibrational state at the internuclear distance x_1 by a strong and ultrashort laser pulse at frequency ω_1 [Fig.1(b)]. If a second continuous-wave laser field at frequency ω_2 is applied to set in resonance the two potential curves at a distance $x_2 > x_1$, a potential well is formed on the adiabatic surface $\mathcal{U}_+(x)$ at the avoided crossing [see Fig.1(b)], and molecular dissociation in thus inhibited in the adiabatic

limit. The nuclear distance x_2 at which the new bond is formed can be tuned by varying the frequency ω_2 of second laser. The optical realization of such a process is shown in Fig.2(a). Here the two slab waveguides have a slowly-varying thickness, linearly decreasing with x for slab S_1 and linearly increasing for slab S_2. The slabs are truncated at $x = x_0$, providing a steep potential barrier for light. An equal slab thickness is reached at $x = x_2 > x_0$. Correspondingly, the potential curves $\mathcal{U}_1$ and $\mathcal{U}_2$ entering in Eqs.(2) mimic the bonding and anti-bonding potential curves of Fig.1(b), with a level crossing at $x = x_2$. Moreover, the coupling rate κ turns out to be nearly independent of x. In our waveguide system, excitation of a dissociating wave packet at $x = x_1$ on the antibonding surface is simply achieved by launching an elliptic Gaussian-shaped beam into the slab S_2 at normal incidence [inset in Fig.2(a)]. Inhibition of molecular dissociation, arising from the formation of an adiabatic trapping well as the coupling strength κ increases, is shown in Figs.2(b)-(d). The integrated intensity light distributions $\int_{S_1} |\psi(x,y,z)|^2 dy \propto |\psi_1(x,z)|^2$ and $\int_{S_2} |\psi(x,y,z)|^2 dy \propto |\psi_2(x,z)|^2$ trapped in the two slabs, shown in Fig.2(b)-(d), are numerically computed by a standard beam propagation analysis of Eq.(1). Note that, for a large waveguide separation [Fig.2(b)], the wave packet on the antibonding curve is accelerated toward increasing values of x and the optical analogue of molecular dissociation is attained. As the waveguide separation decreases (and thus the coupling κ increases), wave packet trapping is clearly observed [Fig.2(d)]. In this case, at the crossing point $x = x_2$ the wave packet periodically tunnels between the two waveguides, and is accelerated in opposite directions

owing to the opposite slopes of the curves $\mathcal{U}_1$ and $\mathcal{U}_2$. This trapping mechanism is imperfect due to Landau-Zener tunneling at each level crossing, and the lifetime of the trapped oscillatory motion increases as κ increases [compare Figs.2(c) and (d)]. The second analogy is the acceleration of a molecular wave packet after a potential crossing due to the dependence of the Landau-Zener transition probability on the wave packet velocity [12]. Let us consider a wave packet that propagates, at a constant speed v_0, along a flat potential curve $\mathcal{U}_1(x) = 0$ and undergoing a Landau-Zener crossing with a second potential curve $\mathcal{U}_2(x) = F(x - x_2)$ at $x = x_2$ [see Fig.1(c)]. In the semiclassical approximation, the wave packet behaves like a particle with a definite momentum $p_0 = n_s v_0$, which is assumed to weakly spread during the crossing and to keep its initial velocity v_0. After the crossing, the probability P_1 of the wave packet to remain on the original potential surface $\mathcal{U}_1$ is given by the usual Landau-Zener formula [9, 12] $P_1 = \exp(-\pi\Lambda)$, where $\Lambda = 2\kappa^2/(|F|\hbar v_0)$. Note that P_1 is larger for a faster wave packet. If the wave packet momentum distribution is broad around its mean p_0, a more complex scenario is found. In particular, owing to the dependence of P_1 on v_0, a filtering effect in the momentum space occurs, with the faster components of the wave packet preferentially remaining on the original potential curve. The final result is a slight increase of the mean wave packet velocity [12]. The analogue of this phenomenon for light beams is shown in Fig.3. Here two slab waveguides, the first one with constant and the second one with a linearly-increasing thickness [Fig.3(a)], mimic the energy crossing scenario of Fig.1(c) with a

force $F \simeq 34$ μm/cm^2 and a coupling $\kappa/\hbar \simeq 1.04$ cm^{-1}. A tilted Gaussian-shaped wave packet $\psi(x, y, 0) = \exp\{-[(y - d/2)/w_y]^2 - [(x - x_1)/w_x]^2 - iv_0 n_s kx\}$, with $w_x = 8$ μm, $w_y = 2.4$ μm, $d = 10.7$ μm, and $x_1 = -800$ μm, excites waveguide S_1 with an initial transverse velocity (refraction angle) $v_0 = 278$ μm/cm, corresponding to a Landau-Zener probability $P_1 \sim 0.48$. Figure 3(b) depicts the path followed by the center of mass $\langle x \rangle$ of ψ_1 (solid line); for comparison, the straight path followed by ψ_1 in absence of slab S_2 is also depicted (dotted curve). The two insets in Fig.3(b) show the the evolution of the fractional beam power $P_1(z)$ of wave packet ψ_1 and its instantaneous velocity $v(z) = d\langle x \rangle/dz$. Note that, as the wave packet reaches the crossing region and light transfer to S_2 starts, the velocity $v(z)$ first decreases from the initial value v_0, then increases and reaches an asymptotic value slightly larger than v_0, indicating an acceleration of the wave packet. Such a behavior can be explained [12] after observing that the faster wave packet components reach first the crossing region and partially tunnel into slab S_2, so that a deceleration of ψ_1 is initially observed. When the slower wave packet components reach the crossing regions, they are partially transferred into slab S_2 and an acceleration of ψ_1 is thus observed. Since the tunneling probability is smaller for the faster wave packet components, the final mean velocity of ψ_1 is larger than the launching one v_0. This effect, however, is small because the change of beam path remains internal to the diffraction cone of the beam [see the shaded area in Fig.3(b)]. Similar behavior is obtained by reversing the slope of the potential $\mathcal{U}_2$.

Optical analogs of coherent phenomena in matters have so far visualized the behavior of the electronic wave function solely [1]. Here a photonic structure capable of mimicking coherent vibrational effects in molecules has been proposed. The present results may stimulate theoretical and experimental studies on optical analogs of coherent vibrational phenomena in molecules or crystals.

Author E-mail address: longhi@fisi.polimi.it

References

1. S. Longhi, "Quantum-optical analogies using photonic structures", Laser & Photon. Rev. **3**, 243 (2009).
2. S. Longhi, M. Marangoni, D. Janner, R. Ramponi, P. Laporta, E. Cianci, and V. Foglietti, "Observation of Wave Packet Dichotomy and Adiabatic Stabilization in an Optical Waveguide", Phys. Rev. Lett. **94**, 073002 (2005).
3. U. Peschel, T. Pertsch, and F. Lederer, "Optical Bloch oscillations in waveguide arrays", Opt. Lett. **23**, 1701 (1998).
4. H. Trompeter, T. Pertsch, F. Lederer, D. Michaelis, U. Streppel, A. Bräuer, and U. Peschel, "Visual observation of Zener tunneling", Phys. Rev. Lett. **96**, 023901 (2006).
5. S. Longhi, M. Marangoni, M. Lobino, R. Ramponi, P. Laporta, E. Cianci, and V. Foglietti, "Observation of Dynamic Localization in Periodically Curved Waveguide Arrays", Phys. Rev. Lett. **96**, 243901 (2006).

6. S. Longhi, G. Della Valle, M. Ornigotti, and P. Laporta, "Coherent Tunneling by Adiabatic Passage in an optical waveguide system", Phys. Rev. B **76**, 201101(R) (2007).

7. Y. Lahini, F. Pozzi, M. Sorel, R. Morandotti, D. N. Christodoulides, and Y. Silberberg, "Effects of nonlinearity on adiabatic light transfer", Phys. Rev. Lett. **101**, 193901 (2008).

8. P. Biagioni, G. Della Valle, M. Ornigotti, M. Finazzi, L. Duò, P. Laporta, and S. Longhi, "Experimental demonstration of the optical Zeno effect by scanning tunneling optical microscopy", Opt. Express **16**, 3762 (2008).

9. B.M. Garraway and K.-A. Suominent, "Wave-packet dynamics: new physics and chemistry in femto-time", Rep. Prog. Phys. **58**, 365 (1995).

10. J.A. Yeazell and T. Uze, *The Physics and Chemistry of Wave-Packets* (Wiley, New York, 2000).

11. J.H. Posthumus, "The dynamics of small molecules in intense laser fields", Rep. Prog. Phys. **67**, 623 (2004).

12. K.-A. Suominent and B.M. Garraway, "Wave-packet dynamics: Level-crossing-induced changes in momentum distribution", Phys. Rev. A **48**, 3811 (1993).

13. A.A. Sukhorukov, Y.S. Kivshar, H.S. Eisenberg, and Y. Silberberg, "Spatial Optical Solitons in Waveguide Arrays", IEEE J. Quant. Electron. **30**, 31 (2003).

14. C. Wunderlich, H. Figger, and T.W. Hänsch, "Ar_2^+ molecules in intense laser

fields", Chem. Phys. Lett. **256**, 43 (1996).

15. L.J. Frasinski, J.H. Posthumus, J. Plumridge, K. Codling, P.F. Taday, and A.J. Langley, "Manipulation of Bond Hardening in H_2^+ by Chirping of Intense Femtosecond Laser Pulses", Phys. Rev. Lett. **83**, 3625 (1999).

List of Figure captions

Fig.1 (Color online) (a) Schematic of a two-slab optical waveguide structure. (b) Nuclear potential energy diagram of a diatomic molecule interacting with two laser fields. (c) Schematic of wave packet splitting at a linear potential energy crossing.

Fig.2 (Color online) (a) Refractive index of the slab waveguide structure that mimics the molecular energy diagram of Fig.1(b). The inset shows the elliptical Gaussian beam that excites guide S_2 at $x = x_1$. (b)-(d): Evolution of light distributions $|\psi_1(x,z)|^2$ (right panels) and $|\psi_2(x,z)|^2$ (left panels) for decreasing values of waveguide separation d: (b) $d = 12$ μm, (c) $d = 9$ μm, (d) $d = 8$ μm. Other parameters are: $\lambda = 633$ nm, $n_s = 1.45$.

Fig.3 (Color online) Wave packet dynamics at a potential crossing. (a) Refractive index of the slab waveguides that mimics the potential crossing of Fig.1(c). (b) Path followed by the center of mass of wave packet ψ_1 (solid curve). The shaded area shows beam spreading. The insets show the evolution of fractional beam power P_1 (bottom) and speed v (top) of wave packet ψ_1.

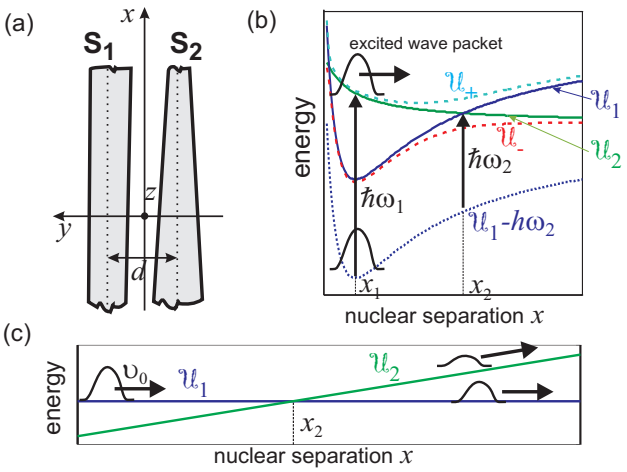
(a)
x
S1
S2
z
y
d
(b)
excited wave packet
energy
ħω1
ħω2
x1
x2
nuclear separation x
(c)
energy
x2
nuclear separation x

Fig. 1.

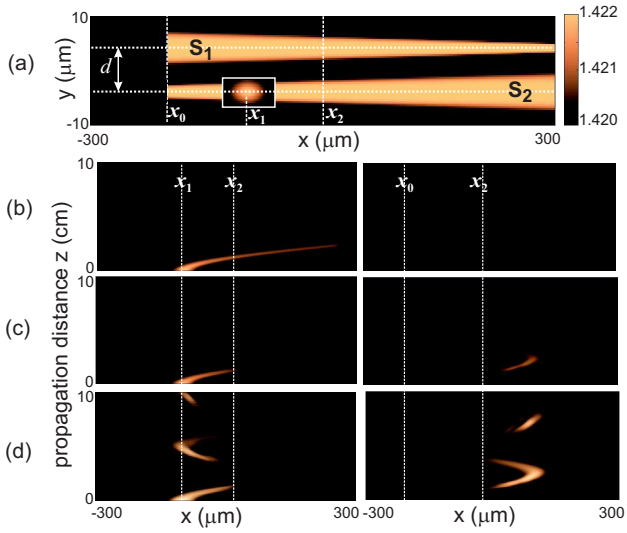
(a)
(b)
(c)
(d)
y (μm)
d
S1
S2
x0
x1
x2
10
-10
-300
300
x (μm)
1.422
1.421
1.420
propagation distance z (cm)
0
10
-300
300
x (μm)

Fig. 2.

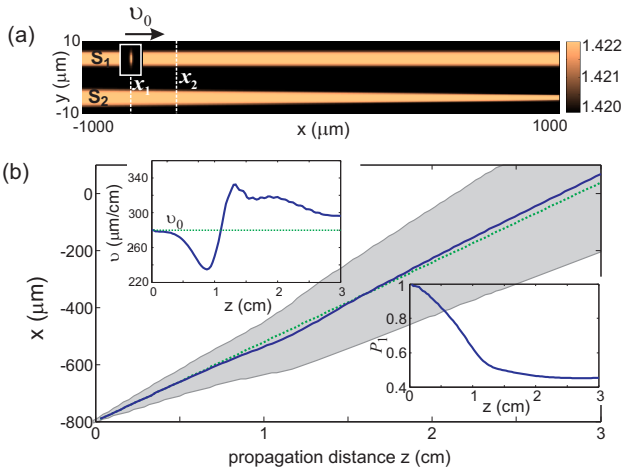
(a)
υ0
10
S1
S2
x1
x2
y (μm)
-10
-1000
x (μm)
1000
1.422
1.421
1.420
(b)
0
-200
-400
-600
-800
x (μm)
υ (μm/cm)
340
300
260
220
υ0
z (cm)
P1
1
0.8
0.6
0.4
propagation distance z (cm)

Fig. 3.